

## Influence of Reaction Time on the Optical Properties of Silver Nanoparticles Synthesized using Soluble Starch

<sup>1,2</sup>Tasi'u, J., <sup>2</sup>Onimisi, M. Y. and <sup>3</sup>Danladi, E.

<sup>1</sup>Department of Physics, Kaduna State University, Kaduna, Nigeria

<sup>2</sup>Department of Physics, Nigerian Defence Academy, Kaduna, Nigeria

<sup>3</sup>Department of Physics, Federal University of Health Sciences, Otuokpo, Benue State, Nigeria

\*Corresponding author's email: [jtikbai@gmail.com](mailto:jtikbai@gmail.com)

### ABSTRACT

Silver nanoparticles (AgNPs) have emerged as promising materials due to their remarkable optical properties, particularly surface plasmon resonance (SPR), which makes them suitable for applications in sensors, catalysis, and optoelectronic devices. However, conventional synthesis methods often involve hazardous chemicals, prompting a shift toward environmentally friendly approaches. This study investigates the optical properties of silver nanoparticles (AgNPs) biosynthesized using soluble starch at various reaction times (30, 60, 90, 120, 150, 180, 240, and 300 minutes). Soluble starch serves as a green, biocompatible reducing and stabilizing agent, enabling the formation of AgNPs under mild conditions. The optical properties of the synthesized nanoparticles were characterized using UV-Visible spectroscopy. The recorded spectra revealed surface plasmon resonance (SPR) absorption bands characteristic of AgNPs, with variations in peak intensity and position corresponding to different reaction times. These findings provide insights into the plasmonic behavior of starch-capped AgNPs and their tunability through reaction duration. The high visible light absorption exhibited by the nanoparticles suggests potential applicability in optoelectronic and photonic devices.

### Keywords:

Silver Nanoparticles,  
Soluble Starch,  
Reaction Time,  
UV-Visible Spectroscopy.

### INTRODUCTION

There has been a tremendous increase in applications utilizing silver nanoparticles (AgNPs) (Silver *et al.*, 2006; Gottschalk *et al.*, 2010). Their distinctive optical properties, coupled with high electrical conductivity, antimicrobial activity, and diverse applications in medicine, electronics, and catalysis, have garnered considerable attention in recent years (Subin *et al.*, 2014; Machado *et al.*, 2015). Silver nanoparticles exhibit strong light absorption and scattering capabilities, which are primarily due to localized surface Plasmon resonance (LSPR)—a phenomenon where conduction electrons undergo collective oscillation in response to incident electromagnetic radiation (Hulteen *et al.*, 1999). Nanoparticles can be made from metals, metal oxides, organic matter, or carbon and range in size from one to one hundred nanometers (Ealia & Saravanakumar, 2017). Various techniques can synthesize silver nanoparticles for research or commercial use, including physical, chemical, and biological processes (Ealia & Saravanakumar, 2017). Biosynthesis of silver

nanoparticles using biological agents offers a sustainable and eco-friendly approach compared to other methods. This technique is safe, cost-effective, and non-toxic (Hasan, 2015). Biological agents such as yeast, algae, bacteria, proteins, phenolic compounds, alkaloids, and other molecules found in plants and microorganisms can facilitate nanoparticle synthesis through reduction, often accomplished in a single step (Nadaroglu *et al.*, 2017). Soluble starch, derived from plants, has shown promise as a stabilizing and reducing agent for the preparation of silver nanoparticles, because it contains various functional groups, including glycosides, alkaloids, steroids, reducing sugars, tannins and flavonoids. Raveendran *et al.* (2003). It is crucial to utilize non-toxic, environmentally friendly, and renewable materials. The concept of preparing green nanoparticles with starch as a stabilizer and as the reducing agent was first presented by Raveendran *et al.* in (2003) (Raveendran *et al.*, 2003; Sobhy & Ashraf, 2015).

The growth and stability of silver nanoparticles can be significantly influenced by varying the reaction time,

which in turn affects their optical properties. Recent studies have explored the impact of different time intervals during the heating process on nanoparticle synthesis. For instance, Tiara et al. (2020) conducted a study on the biosynthesis of AgNPs, in which they varied the volume ratio of plant extract to silver nitrate ( $\text{AgNO}_3$ ) at 5.0:1, 2.0:1, 0.5:1, 0.2:1, and 0.1:1, across multiple reaction times—specifically 25 minutes, 2, 3, 24, 48, and 96 hours. According to Ravichandran et al. (2011), a common method for synthesizing silver (Ag) nanoparticles involves the addition of leaf extract to an aqueous  $\text{AgNO}_3$  solution in an Erlenmeyer flask, followed by heating in a water bath at  $75^\circ\text{C}$  for 60 minutes. Similarly, Abha et al. (2017) reported that a 1 mM of  $\text{AgNO}_3$  solution was added to the plant extract under constant stirring. The reaction mixture was monitored for a color change at four various time intervals 2, 4, 6, and 24 hours. Additionally, Joud et al. (2021) investigated the effect of reaction time on silver nanoparticle production, examining durations of 24, 48, and 72 hours. While several studies have explored this effect using plant extracts, there is limited research on how reaction time affects AgNP synthesis when using soluble starch as a green reducing and stabilizing agent. This study aims to fill that gap by investigating the influence of different reaction times (30-300minutes) on the growth and stability of AgNPs produced with soluble starch. The findings will contribute to the development of novel and efficient synthesis methods, as well as enhance our understanding of the fundamental properties of silver nanoparticles in general. UV-Visible spectrophotometry was employed to monitor the progression of the reaction, providing insight into the development and optical characteristics of the synthesized nanoparticles.

## MATERIALS AND METHODS

### Materials

The materials utilized in this study comprise soluble starch powder, silver nitrate ( $\text{AgNO}_3$ ), glassware, distilled water, deionized water, a magnetic stirrer, a hotplate, beakers, and a UV-visible spectrophotometer. All chemicals employed are of high purity and sourced from Solaronix. The glassware was thoroughly cleaned with  $\text{HNO}_3$  and distilled water, then dried using a hot blower.

### Preparation of the of silver nanoparticle

In a standard one-step synthesis procedure, 0.5 g of soluble starch was dissolved in 50 mL of deionized water and gently heated with stirring on a hotplate at  $70^\circ\text{C}$  for 30 minutes to produce silver nanoparticles (AgNPs). The mixture later received 0.1g of  $\text{AgNO}_3$  and was allowed to boil for 8 different interval of time (30, 60, 90, 120, 150, 180, 240 and 300 minutes) on a hotplate while being stirred. To prevent particles from falling during the procedure, the beaker was covered with foil paper. The color of the silver nitrate solution changed from colorless to brownish yellow, which was visible to the naked eye. The resulting AgNPs were purified by centrifuging several times for 20 minutes at 1,000 rpm, followed by rinsing with distilled water. The AgNPs were then collected and redispersed in deionized water for further characterization. The optical properties of the AgNPs were analyzed using UV-visible spectroscopy. The processes of the biosynthesized silver nanoparticle are shown in Figure 1.

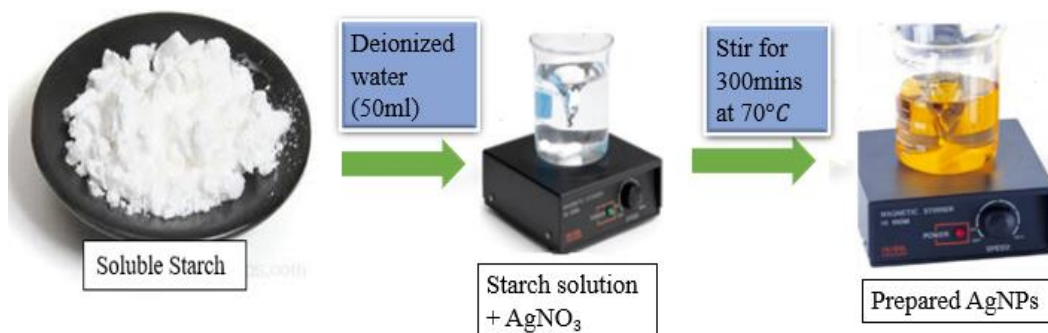


Figure 1: Process of bio-synthesized AgNP using soluble starch

### Characterization and Measurement

The characterization of silver nanoparticles was done by UV-Vis spectroscopy (UV752 UV-Vis-NIR spectrophotometer). The optical absorbance, transmittance, reflectance and bandgap of prepared AgNPs at different interval of time (30, 60, 90, 120, 150, 180, 240 and 300min) were determined. UV-Visible

spectroscopy is commonly the initial technique employed for characterizing metallic nanoparticles due to the surface Plasmon resonance (SPR) phenomenon (Shankar et al., 2013). The measurement was performed at room temperature within the wavelength range of 200-1200 nm.

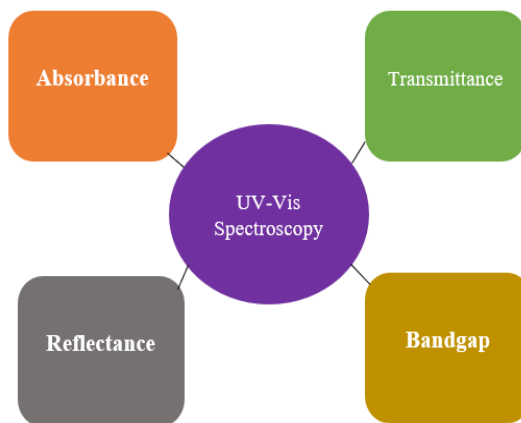


Figure 2: Several UV-Spec characterizations of the prepared AgNPs

**RESULT AND DISCUSSION**

The Optical absorbance, reflectance, transmittance and bandgap of AgNPs at different interval of time are presented in Figure 3(a-d).

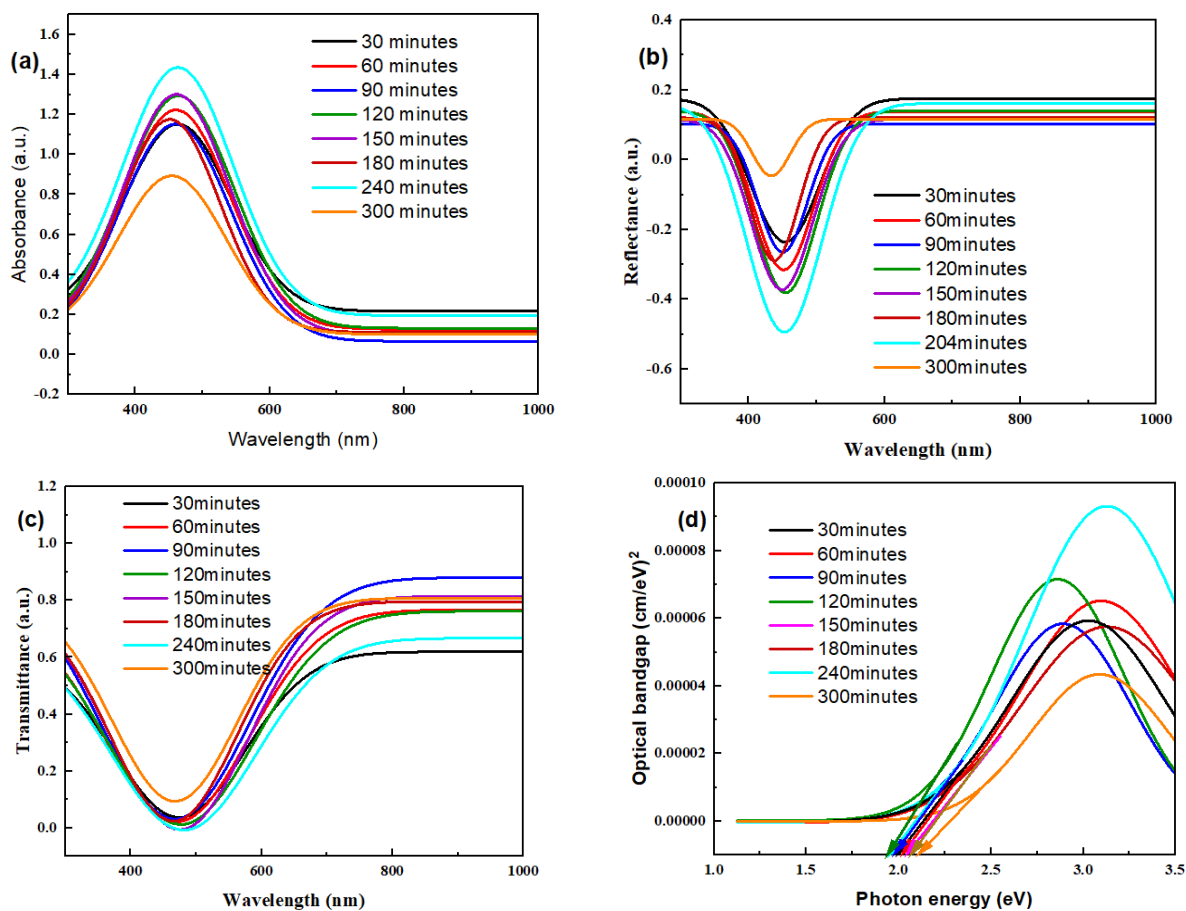


Figure 3: Optical (a) absorbance (b) reflectance (c) transmittance and (d) bandgap of AgNPs at different interval of time

The absorbance of the prepared AgNPs is shown in Figure 3(a). According to the figure, the material absorbed light between 400 and 800 nm, with absorption peaks seen between 450 and 470 nm. This material meets the criteria for use as a light harvester, as demonstrated by its absorption in the visible region. Numerous studies have indicated that the absorption band between approximately 200–800 nm is ideal for characterizing particles ranging in size from 2 to 100 nm (Malliga et al., 2014). The figure illustrates that the absorption peak becomes more pronounced as the time increases from 30 to 240 minutes. This shows that initially, poly dispersed AgNPs are formed, and as reaction time increases, monodispersed spherical nanoparticles are formed. Therefore, the duration of mixing at room temperature plays a crucial role in influencing the size distribution of AgNPs (Malliga et al., 2014). The Ag nanoparticle film's optical absorption spectrum demonstrates that the wavelength increases (the red shift) as the Ag nanoparticle's diameter increases because the width of the surface plasma peak widens. As observed from Figure 3(a), AgNPs@240minutes has the highest absorption peaks, with absorption peaks of 448.33nm.

Figure 3(b) displays the optical reflectance of AgNPs at various time intervals. The samples were found to be relatively reflective, as shown by the graph. AgNPs were left on for longer periods of time, and a decrease in reflectance was seen. Reflectance increased gradually from 588 nanometers to a maximum peak at 672 nanometers, after which peaks and valleys emerged. According to Jinhui et al. (2021). This increase in reflectance is attributed to the enhanced surface roughness.

The optical transmittance of AgNPs at various time intervals is depicted in Figure 3(c). For optical fabrication purposes, the crystal must exhibit high transparency across a significant wavelength range (Shankar et al., 2013). In the visible and near-infrared spectrums, all samples have high transparency; however, a sharp decrease in transparency is seen in the ultraviolet spectrum. A significant decrease in transmittance was seen above 800 nm and below 600 nm ranges. The observed variations in the sample's transmittance are attributed to variations in their surface morphology, crystallite sizes, and the presence of surface defects that cause a reduction in transmittance due to light scattering (Feng et al., 2018).

The bandgap is an essential parameter in determining the nanoparticles' conductivity, optical absorption, and emission properties. A smaller bandgap indicates enhanced electrical conductivity and absorption in the visible light range, whereas a larger bandgap suggests the nanoparticles' ability to absorb higher-energy photons, extending their applications into the UV range (Mbamara et al., 2024).

Equation (1), which Tauc proposed in 1966, is the basis on which the optical bandgap energy is calculated. Each tangent to the x-axis at  $y=0$  yields the optical bandgap. The optical bandgap can be determined using the relationship in accordance with absorption theory (Mat et al., 2022).

$$(\alpha hv) = B(hv - E_g)^n \quad (1)$$

Here, B is a constant,  $\alpha$  represents the absorption coefficient,  $E_g$  is the bandgap energy, and  $v$  denotes the transition frequency. The exponent  $n$  is a numerical constant that defines the nature of the band transition: values of  $n = 1/2$  and  $3/2$  indicate directly allowed and directly forbidden transitions, while  $n = 2$  and  $3$  correspond to indirectly allowed and indirectly forbidden transitions, respectively.

The bandgap can be estimated by extrapolating the linear portion of the  $(\alpha hv)^2$  versus photon energy ( $hv$ ) plot for a direct bandgap, or the  $(\alpha hv)^{1/2}$  versus photon energy ( $hv$ ) plot for an indirect bandgap. Here,  $\alpha$  is the absorption coefficient, which can be calculated from the absorption spectrum using the following equation

$$\alpha = \frac{2.303A}{d} \quad (2)$$

Where  $d$  is the thickness and  $A$  is the absorbance.

It can be observed from figure. 3(d) that the samples have a direct bandgap of 2.06, 1.96, 1.91, 1.94, 2.09, 1.99, 2.11 and 2.16 eV for 30, 60, 90, 120, 150, 180, 240 and 300min, respectively. These values represent the energy gap between the valence band and the conduction band of the biosynthesized silver nanoparticles. The bandgap values decrease and increase at different time intervals, indicating variations in the optical properties and electronic transitions of the nanoparticles.

The observed variation in bandgap values during the biosynthesis process at different time intervals indicates changes in particle size, morphology, crystallinity, and composition. These variations can be attributed to the growth kinetics, reduction rate, interaction with stabilizing agents, and other factors influencing the synthesis process.

## CONCLUSION

Silver nanoparticles were successfully synthesized using a green method, with soluble starch acting as a reducing and stabilizing agent at various reaction times (30, 60, 90, 120, 150, 180, 240, and 300 minutes). The optical properties of the synthesized nanoparticles were characterized using UV-Visible spectroscopy, which confirmed the formation of AgNPs through the observation of surface plasmon resonance (SPR) bands. The strong absorption in the visible region exhibited by the samples suggests their potential suitability for optoelectronic applications.

## REFERENCES

- Abha V., Tyagi, S., Verma, A., Singh, J., & Joshi, P. (2017). Optimization of different reaction conditions for the bio-inspired synthesis of silver nanoparticles using aqueous extract of *Solanum nigrum* leaves. *Journal of Nanomaterials & Molecular Nanotechnology*, 6(2). <https://doi.org/10.4172/2324-8777.1000214>
- Ealia, A. M., & Saravanakumar, M. P. (2017). A review on the classification, characterisation, synthesis of nanoparticles and their application. In *IOP Conference Series: Materials Science and Engineering*, 263(3), 032019. IOP Publishing. <https://doi.org/10.1088/1757-899X/263/3/032019>
- Feng, A., Cao, J., Wei, J., Chang, F., Yang, Y., & Xiao, Z. (2018). Facile synthesis of silver nanoparticles with high antibacterial activity. *Materials*, 11(12), 2498. <https://doi.org/10.3390/ma11122498>
- Gottschalk, F., Sonderer, T., Scholz, R. W., & Nowack, B. (2010). Possibilities and limitations of modeling environmental exposure to engineered nanomaterials by probabilistic material flow analysis. *Environmental Toxicology and Chemistry*, 29(5), 1036–1048. <https://doi.org/10.1002/etc.150>
- Hasan, S. (2015). A review on nanoparticles: Their synthesis and types. *Biosynthesis: Mechanism*, 4, 9–11.
- Hulteen, J. C., Treichel, D. A., Smith, M. T., Duval, M. L., Jensen, T. R., & Van Duyne, R. P. (1999). Nanosphere lithography: Size-tunable silver nanoparticle and surface cluster arrays. *The Journal of Physical Chemistry B*, 103(19), 3854–3863. <https://doi.org/10.1021/jp9904771>
- Jinhui, T., Jiang, Q., Zhang, F., Kang, S. B., Kim, D. H., & Zhu, K. (2021). ACS Energy Letters, 6, 232–248. <https://doi.org/10.1021/acseenergylett.0c02105>
- Joud, J., Wassim, A., Adawia, K., & Rawaa, A. (2021). Green synthesis of silver nanoparticles using aqueous extract of *Acacia cyanophylla* and its antibacterial activity. *Heliyon*, 7(6), e08033. <https://doi.org/10.1016/j.heliyon.2021.e08033>
- Machado, S., Pacheco, J. G., Nouws, H. P. A., Albergaria, J. T., & Delerue-Matos, C. (2015). Characterization of green zero-valent iron nanoparticles produced with tree leaf extracts. *Science of The Total Environment*, 533, 76–81. <https://doi.org/10.1016/j.scitotenv.2015.06.087>
- Malliga, P., Pandiaraja, J., & Prithivikumar, N. (2014). Influence of film thickness on structural and optical properties of sol-gel spin coated TiO<sub>2</sub> thin film. *IOSR Journal of Applied Physics*, 6(1), 22–28. <https://doi.org/10.9790/4861-06112228>
- Mat Yunin, M. Y. A., Mohd Adenan, N., Khairul, W. M., Yusoff, A. H., & Adli, H. K. (2022). Effect of stability of two-dimensional (2D) aminoethyl methacrylate perovskite using lead-based materials for ammonia gas sensor application. *Polymers*, 14(9), 1853. <https://doi.org/10.3390/polym14091853>
- Mbamara, C., Nworie, I. C., Brown, N. W., Otah, P. B., Oko, K. I., Idu, H. K., & Amadi, M. C. (2024). Synthesis and Characterization of Nickel-Doped Cerium Oxide Thin Films Using Solution Growth Technique. *Nigerian Journal Physics*, 33(4), 139–146. <https://doi.org/10.62292/njp.v33i4.2024.334>
- Nadaroglu, H., Alayli, A. G., & Ince, S. (2017). Synthesis of nanoparticles by green method. *International Journal of Innovative Research and Review*, 1(1), 6–9.
- Raveendran, P., Fu, J., & Wallen, S. L. (2003). Completely “green” synthesis and stabilization of metal nanoparticles. *Journal of the American Chemical Society*, 125(46), 13940–13941. <https://doi.org/10.1021/ja029267j>
- Ravichandran, V., Tiah, Z. X., Subashini, G., Terence, F. W. X., Eddy, F. C. Y., Nelson, J., & Sokkalingam, A. D. (2011). Biosynthesis of silver nanoparticles using mangosteen leaf extract and evaluation of their antimicrobial activities. *Journal of Saudi Chemical Society*, 15(2), 113–120. <https://doi.org/10.1016/j.jscs.2010.06.004>
- Shankar, G., Joseph, P. S., Yosuva Suvakin, M., & Sebastiyam, A. (2013). Optical reflectance, optical refractive index and optical band gap measurements of nonlinear optics for photonic applications. *Optics Communications*, 295, 134–139. <https://doi.org/10.1016/j.optcom.2012.12.011>
- Silver, S., Phung, L. T., & Silver, G. (2006). Silver as biocides in burn and wound dressings and bacterial resistance to silver compounds. *Journal of Industrial Microbiology & Biotechnology*, 33(7), 627–634. <https://doi.org/10.1007/s10295-006-0139-7>
- Sobhy, M. Y., & Mostafa, A. A. (2015). A novel green synthesis of silver nanoparticles using soluble starch and its antibacterial activity. *International Journal of Clinical and Experimental Medicine*, 8(3), 3538–3544.
- Subin, P., Tapobrata, P., Praseetha, P. N., & Thomas, T. (2014). Biosynthesis of silver nanoparticles. *Journal of Nanoscience and Nanotechnology*, 14(3), 2038–2049. <https://doi.org/10.1166/jnn.2014.8403>
- Tiara, E. A., Handayani, W., & Imawan, C. (2020). The UV-Vis spectrum analysis from silver nanoparticles synthesized using *Diospyros maritima* Blume leaves extract. In *Advances in Biological Sciences Research*. 14, 411–419. <https://doi.org/10.2991/absr.k.210621.070>